Wang *et al. Biochar* (2025) 7:55
https://doi.org/10.1007/s42773-025-00444-4

Biochar

ORIGINAL RESEARCH Open Access

Insights into the interfacial dynamics and interaction mechanisms between phosphate-solubilizing bacteria and straw-derived biochar

Zhe Wang[1,2], Bing Chen[2*], Yiqi Cao[2], Sufang Xing[1], Baiyu Zhang[2], Shuguang Wang[1,3,4] and Huifang Tian[1*]

Abstract

To alleviate soil phosphorus deficiency, integrating straw-derived biochar with phosphate-solubilizing bacteria (PSB) has been recognized as a promising solution and is gaining growing attention. However, the mechanisms of bacterial immobilization and the influences of the physicochemical attributes of biochar remain unclear. In this study, we investigated the single-cell interactions of gram-negative *Acinetobacter pittii* and gram-positive *Bacillus subtilis* with cotton straw-derived biochars, subjected to progressively increasing pyrolysis temperatures, to understand the attributes of gradually modified biochar properties. The results revealed the correlations between adhesion forces and biochar properties (e.g., surface area and surface charge), and the strongest adhesion for both strains for the biochar pyrolyzed at 700 °C. The extended Derjaguin-Landau-Verwey-Overbeek (XDLVO) model, structured to predict interaction energy, was subsequently compared with experimental observations made using atomic force microscopy (AFM). Discrepancies between the predicted high adhesion barriers and the observed attraction suggested that forces beyond Lifshitz-van der Waals also influenced the immobilization of PSB. Adhesion-distance spectroscopy and XDLVO theory jointly revealed four distinct phases in the immobilization process by biochar: planktonic interaction, secondary minimum entrapment, primary barrier transcendence, and initial reversible adherence, collectively facilitating biofilm formation. Notably, initial reversible adhesion positively correlated with increased protein and polysaccharide levels in extracellular polymeric substances (EPS) ($R^2 > 0.67$), highlighting its importance in biofilm formation. Unraveling PSB–biochar interactions can improve the effectiveness of soil inoculants, thereby enhancing phosphorus availability in soil, a crucial factor for promoting plant growth and supporting environmental sustainability.

Highlights

- Phosphate-solubilizing bacteria adhere to biochar in water, improving nutrient availability and soil health.
- Bacteria overcome energy barriers through synergistic interactions, which enhances their adhesion to biochar surfaces.
- High-temperature biochar increases bacteria immobilization and adhesion, boosting EPS production and stability.

*Correspondence:
Bing Chen
bchen@mun.ca
Huifang Tian
hftian@sdu.edu.cn
Full list of author information is available at the end of the article

Keywords Phosphate-solubilizing bacteria, Cotton straw-derived biochar, Reversible adhesion, Bacterial immobilization, Interfacial dynamics, Bacterial interactions

Graphical Abstract

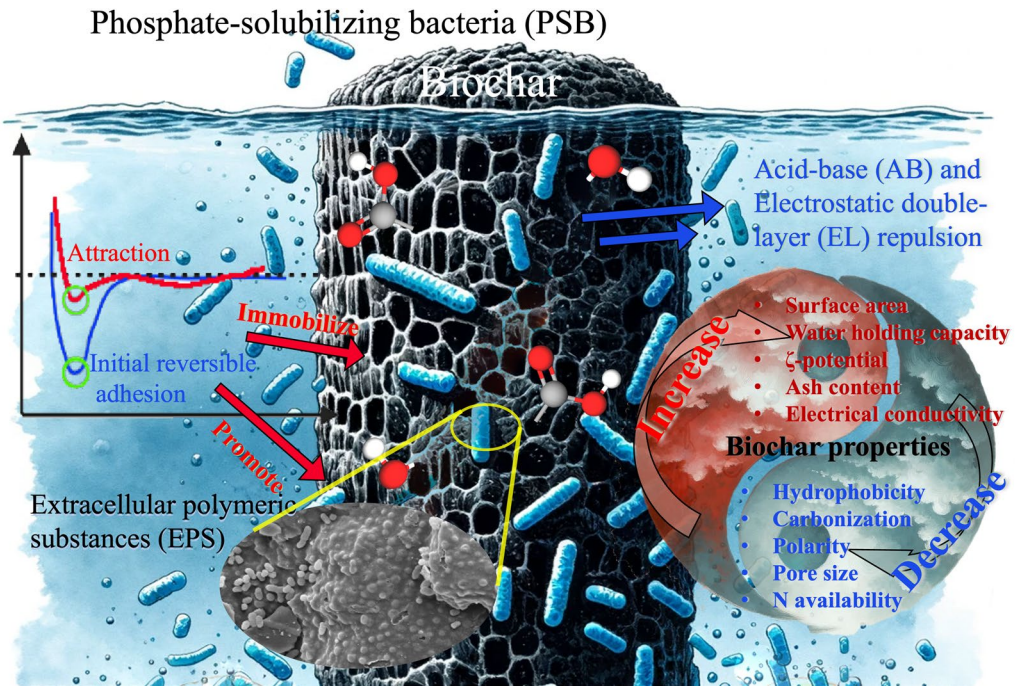

1 Introduction

The soil environment teeming with diverse organisms is the foundation for agriculture and terrestrial ecosystems. Phosphorus, a vital nutrient for plant growth, is critical in energy transfer and the synthesis and metabolism of nucleic acids and cell membranes (MacDonald et al. 2011). In highly weathered or poorly managed soils, bioavailable phosphorus is often scarce, leading to the excessive use of artificial phosphorus fertilizers (Shrestha and Wang 2020). This excessive use, compounded by conditions such as excessive irrigation or intense rainfall, can cause phosphate to leach into water bodies, degrading water quality, exacerbating algal blooms, and disrupting aquatic ecosystems. This deficiency limits plant productivity (MacDonald et al. 2011), affects atmospheric carbon dioxide sequestration, and destabilizes microbial dynamics (Hartmann and Six 2023), potentially reducing crop yields.

Phosphate-solubilizing bacteria (PSB) are essential for enhancing phosphate bioavailability in soil by converting inaccessible phosphates into forms absorbable by plants (Zheng et al. 2019). Studies have identified both gram-positive bacteria (e.g., *Bacillus megaterium* (Wang et al. 2022), *Bacillus subtilis* (Toro et al. 1997), and *Streptomyces prasinopilosus* (Zheng et al. 2019)) and gram-negative bacteria (e.g., *Pseudomonas frederiksbergensis* (Zheng et al. 2019), and *Acinetobacter pittii* (Zhao et al. 2023)) as PSBs. Gram-positive bacteria are distinguished from gram-negative bacteria by their extensive peptidoglycan layer, which carries an elevated charge density due to the presence of teichoic acids (Adam et al. 2023); gram-negative bacteria have a comparatively thin peptidoglycan layer and feature an outer membrane rich in lipopolysaccharides (Weidenmaier and Peschel 2008). These structural differences may result in distinct bacteria-environment interactions. While bacterial structural differences provide crucial insights into their potential interactions within various environments, the effectiveness of these bacteria often hinges on their delivery methods. Particularly, liquid bacterial inoculants, widely used in environmental and agricultural applications, face significant challenges. These inoculants generally exhibit short-term effectiveness and are vulnerable to

environmental stresses like desiccation, nutrient scarcity, and temperature fluctuations, which can rapidly reduce PSB populations and undermine the long-term success of inoculations in field conditions (Trimurtulu et al. 2014; Wang et al. 2022). Research has shown that incorporating a carrier material providing a supportive matrix enhances the viability and functional efficacy of bacterial inoculants (Sun et al. 2016). This approach has addressed the challenges associated with direct applications, mitigating declines in PSB populations and nutrient availability.

Biochar, known for its unique features like surface functional groups and porosity (Das 2024), is acclaimed for its ability to mitigate soil nutrient deficiencies (Mukherjee et al. 2022) and enhance soil quality through improved microbial adherence and metabolism (Xiang et al. 2022). By providing a protective habitat with its porous structure and varied surface chemistry, biochar significantly improves microbial adherence and metabolism. It is shown that the common practice of open burning straw waste in China leads to soil degradation and greenhouse gas emissions (Meng et al. 2019). Research on converting agricultural waste into valuable straw biochar through energy-efficient pyrolysis is thus necessary, as it is cost-effective, environmentally sustainable, and suitable for large-scale production, helping stabilize and sequester carbon in the soil to mitigate climate change impacts (Vijay et al. 2021; Wang et al. 2013). Further, incorporating straw biochar with functional bacteria not only enhances bacterial vitality but also increases their functional efficacy (Huang et al. 2023). This process enhances soil properties by improving pH levels and increasing nutrient availability (Zhang et al. 2023), and promotes a circular economy by reducing waste disposal costs. Further, the performance of straw-biochar surpasses natural materials like clay in supporting microbial activity and stabilizing pollutants and it remains cost-effective compared with graphene (Liang et al. 2023), making it a promising option for environmental applications.

The unique woody structure and high cellulose and lignin content of cotton straw, akin to traditional woody biomass such as sawdust, make it an excellent candidate for biochar production (Kristoferson and Bokalders 1986; Patil et al. 2007). These constituents contribute to the formation of a stable and porous biochar structure, facilitating bacterial colonization and retention, thereby enhancing the efficacy of soil amendments (Xu et al. 2014). Additionally, compared with other crop straws, cotton straw has a clear advantage in large yield, providing a sustainable, low-cost, and widely available resource for biochar production (Lehmann and Joseph 2024). Moreover, biochar prepared from cotton straw has characteristics of higher carbon content, larger surface area, better variable nutrient availability, and a more resilient structure, which contribute to increased microbial colonization by improving nutrient availability, providing better microbial support, and sustaining bacterial communities, particularly in nutrient-poor soils (Lehmann et al. 2011). Further, a previous study demonstrating sustained PSB activity in cotton straw-derived biochar in soil highlights its effectiveness and versatility as a carrier (Wang et al. 2022). However, the determinants and underlying mechanisms of cotton straw-derived biochar as a carrier for immobilizing PSB remain incompletely understood. Primary uncertainty stems from the behavior of externally inoculated microorganisms. During the inoculant preparation phase, functional exogenous bacteria are deliberately incorporated, allowing for reversible and vulnerable attachment (Eskhan and Johnson 2022), which leaves them prone to detachment before immobilization on the substrate (Costa et al. 2011). In the reversible adhesion phase, the predominant interactions are assumed to be nonspecific, primarily involving van der Waals forces and hydrophobic interactions between the bacteria and substrate (Vigeant et al. 2002). Following reversible adhesion, a conditioning biofilm layer forms, comprising organic components such as proteins, glycoproteins, lipids, nucleic acids, polysaccharides, and humic substances (Costa et al. 2011). Subsequently, cells progress to the irreversible attachment phase, making biochar an effective vector for immobilizing microorganisms (Mukherjee et al. 2022). A significant research gap persists in elucidating the interfacial dynamics that govern PSB attachment to biochar. Addressing this gap is crucial for enhancing our understanding of the immobilization process.

Previous studies have established a groundwork for exploring interfacial dynamics. Employing atomic force microscopy (AFM), Mittelviefhaus et al. (2019) discerned a correlation between hydrophobicity and bacterial adhesion to leaf surfaces, highlighting the importance of hydrophobic interactions in plant disease etiology. Wang et al. (2019) used extended Derjaguin-Landau-Verwey-Overbeek (XDLVO) theory to demonstrate how chemical aging amplifies repulsion between biochar colloids and sand, implicating changes in hydrophilicity and Lewis acid–base interaction energy. Insights from these studies emphasized the complexity of surface interactions in environmental and biological systems.

Capitalizing on these insights, the present study sought to understand the interfacial dynamics between two structurally distinct PSB strains (*Acinetobacter pittii* and *Bacillus subtilis*) and cotton straw-derived biochars with various physicochemical properties. Using single-cell force spectroscopy (SCFS) through AFM and quantifying

key extracellular polymeric substances (EPS), this research uncovered the underlying adhesive interactions experimentally. We applied the XDLVO modeling as a theoretical framework to offer insights into the energy/force profiles that govern bacterial-biochar interactions, resulting in immobilization. This dual research strategy aimed to decipher complex mechanisms of bacterial immobilization, where each method compensated for the limitations of the other. The primary aim of this study was to provide an improved scientific understanding of the associated mechanisms, particularly by elucidating the interfacial dynamics between PSB and biochar and the crucial factors governing their interactions. The insights gained could help enhance bacterial immobilization and potentially refine biochar application strategies, thereby increasing its effectiveness in soil amendments. A deeper understanding of PSB immobilization on biochar facilitates agricultural residue reclamation strategies and boosts nutrient cycling and environmental remediation. With future efforts focused on testing and demonstrating their applicability, these advances are ultimately expected to benefit environmental sustainability and foster the development of more sustainable agricultural practices.

2 Materials and methods

2.1 Preparation and characterization of biochars

When the pyrolysis temperature for biochar preparation exceeds 700 °C, it significantly reduces biochar yield. We selected this temperature range to balance energy efficiency and product output, addressing both economic and practical considerations (Ahmed et al. 2016; Zhang et al. 2015). Therefore, biochars were produced from cotton straw at temperatures ranging from 200 °C to 700 °C, with increments of 100 °C. The resulting biochar products were designated as CS200, CS300, CS400, CS500, CS600, and CS700, corresponding to the respective pyrolysis temperatures. Details and specifications regarding the preparation process are available in the Supporting Information (Text S1).

Brunauer–Emmett–Teller (BET) analysis was employed to determine the surface area, total pore volume, and porosity analysis of biochar using the Surface Area and Porosity Analyzer (ASAP 2460, Micromeritics, USA). The pH and electrical conductivity were determined in a biochar/water slurry at a 1:10 (w/v) ratio with a pH meter (FE28-Standard, Mettler Toledo, Switzerland) and an electrical conductivity meter (DDSJ-308A, YANTAI Stark Instrument Co., LTD, China). Contact angles were assessed by a contact angle system (HARKE-SPCA, Beijing Harke Test Instrument Factory, China). In the Supporting information, detailed descriptions of the biochar ash content, water holding capacity, and elemental composition measurements are provided in Text S1. Please refer to Text S2 for comprehensive information about the bacteria contact angle measurements. Each parameter was selected to evaluate specific physicochemical properties of the biochar, which are essential for determining its interaction with PSB.

2.2 Selection of PSB

Two commonly used PSB strains were selected for this study: *Bacillus subtilis* OP-8, isolated from soil by Liu et al. (2020) at Shandong University, and *Acinetobacter pittii* CICC 10526, acquired from the China Center of Industrial Culture Collection (CICC). *B. subtilis* and *A. pittii* are recognized for their robust phosphate-solubilizing capabilities, effective in diverse soil environments (Swain et al. 2012), and adept at solubilizing various phosphorus sources (Wan et al. 2020), demonstrating their versatility across different conditions. To assess their phosphate-solubilizing capabilities, a comparative analysis was conducted between these strains and *Bacillus megaterium*, known for its significant phosphate solubilization ability (Wang et al. 2022). The detailed methodology and results regarding the phosphate-solubilizing capacity of the bacterial strains, their cultivation, available phosphorus quantification, and the assessment of bacterial hydrophobicity are provided in the Supporting Information (Text S3).

2.3 Characterization of biochar immobilized with PSB

Fourier Transform Infrared Spectroscopy (FTIR) (Nicolet iS50, Thermo Fisher, USA) was utilized to analyze the surface chemistry of both pristine biochars and biochar-PSB inoculants. Measurements across the mid-infrared region (4000–400 cm^{-1}) were specifically chosen to accurately identify functional groups that play a critical role in biochar–PSB interactions. Zeta potential measurement of biochars and bacteria was conducted using a Zetasizer 3000HSA (Malvern Co., UK) to determine electrophoretic mobility, which was then converted via the Smoluchowski equation. This method was selected to assess the surface charge properties of the biochars and bacteria, crucial for understanding their stability and interaction dynamics in aqueous environments. Additionally, Scanning Electron Microscopy (SEM) (Quanta 250 FEG, USA) was employed to visualize the physical structures and morphological characteristics of both pristine biochars and various biochar-immobilized PSB strains.

2.4 Bacterial immobilization on biochar

To evaluate the effectiveness of bacterial immobilization, bacterial cells from two PSB strains were washed with sterilized saline solution during their logarithmic phase.

For soil remediation inoculant purposes, bacterial concentrations ranging from 10^7 to 10^9 colony-forming units (CFU) per gram of biochar are typically used for immobilizing different bacteria (Głodowska et al. 2017; Sun et al. 2016). Acknowledging that higher bacterial concentrations do not necessarily lead to improved immobilization, the study evaluated the effectiveness of immobilization across varying concentrations of inoculated bacteria. Concentrations of 1×, 2×, 3×, 4×, and 5×solutions were subsequently prepared through centrifugation and dilution, with the 1×solution yielding a bacterial concentration of 3×10^7 CFU mL^{-1}. These solutions were then employed to ascertain the maximum immobilization of each PSB strain. To quantify cells not immobilized by biochar, the natural sedimentation method was employed to segregate biochar and free cells. The supernatant containing non-immobilized cells was carefully collected, and the CFU of free cells was determined using standard plating techniques. Details of the experimental setup and the procedure for preparing bacteria immobilized on biochar are provided in the Supporting Information (Text S4).

2.5 EPS matrix extraction and characterization

Polysaccharides and proteins, as the principal constituents of EPS (Zhang et al. 2021), were quantified in this study. Bacterial cells were cultivated in LB liquid medium to reach a consistent concentration of CFU mL^{-1} during their mid-exponential phase. Sterilized biochar was added to the culture at a 100:1 (v/w) ratio of biochar to liquid medium, and comparison groups were established without biochar. This step isolates specific interactions between the PSB and the biochar, minimizes confounding factors from other microorganisms, and controls experimental variables effectively. The mixture was then inoculated with the bacterial culture at a 1% (v/v) concentration. This setup initiated the experiment, which continued for five days to promote substantial EPS development. The selected ratios of biochar to medium and bacterial inoculation were designed to maximize bacterial interactions and enhance EPS production. All samples were cultivated in a shaker incubator for 5 days. The polysaccharide content of EPS was determined using the anthrone-sulfuric acid method, with glucose serving as the reference standard (Gaudy 1962). The total protein content in the extracted EPS was quantified using a Bicinchoninic Acid (BCA) kit (Nanjing Jiancheng Bioengineering Institute, China) with bovine serum protein as the standard.

2.6 Adhesion-distance spectroscopy measurements

The AFM was used to quantify the interfacial forces between a cell and its underlying substrate (Eskhan and Johnson 2022). Using AFM, the approach curve offers crucial insights into the pre-contact interactions by delineating the forces at play. Alongside this, the retraction curves, which quantify the strength of reversible adhesion, contribute to a thorough understanding of the contact initiation phase at the nano-scale.

Figure 1 illustrates the modified protocol for creating a colloidal probe for SCFS using AFM (Nanowizard 4, Bruker, Germany) from Beaussart et al. (2014). Briefly, silica beads with a diameter of 5 μm were affixed to tipless cantilevers (MLCT-O10 from Bruker, Germany) using AB epoxy adhesive (Fig. 1a and b). Proper assembly of the probe and the central positioning of the bead were confirmed visually. A single viable PSB cell, stained with the LIVE/DEAD BacLight viability kit (Invitrogen, kit no. L7012), was adhered to the silica bead, visible as green fluorescence under a fluorescent microscope (IX73, Olympus, Japan) (Fig. 1c). Adhesion force measurement between PSB cells and various biochar substrates was conducted immersed in 1×PBS solution (pH 7.4, ionic strength 0.15 M) at 25 °C to simulate the conditions of PSB-biochar inoculant preparation (Chai et al. 2022). Adhesion forces of individual PSB cells interacting with different biochar substrates were quantified by recording over 200 force-distance curves using atomic force microscopy in contact mode. Corresponding measurements for cell-free probes served as controls. The absolute value of the minimum force recorded during the retraction of probe signifies the adhesion force (Fig. 1d). Details on probe coating and calibration are provided in Supporting Information (Text S5).

2.7 Extended Derjaguin-Landau-Verwey-Overbeek (XDLVO) interaction energy and force prediction

The XDLVO model investigates particle interactions in liquids, considering Lifshitz-van der Waals (LW), electrostatic double-layer (EL), and acid–base (AB) forces. These combined forces offer a comprehensive view of the interaction energy and particle behavior in fluids (Liu et al. 2010). Given that the sizes of PSB cells are considerably smaller than those of biochar particles (≤0.149 mm), it is reasonable to assume that PSB cell surfaces are spherical and biochars are plate-like in shape. The model assumes that the cells are spherical and that their interactions possess both additive and non-retarded characteristics (Hamaker 1937).

$$\phi_{bwp}^{XDLVO} = \phi_{bwp}^{LW} + \phi_{bwp}^{EL} + \phi_{bwp}^{AB}$$

where ϕ_{bwp}^{XDLVO} represents the total interaction energy between biochar substrate and bacteria immersed in 1×PBS solution, ϕ_{bwp}^{LW} is the component attributed to the

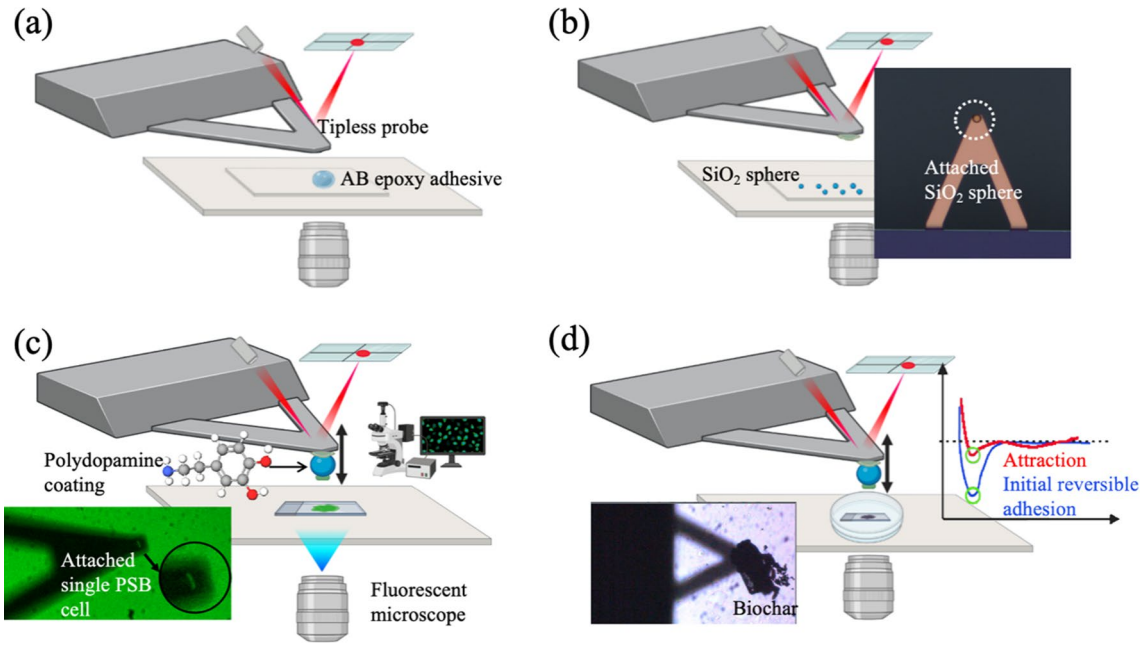

Fig. 1 Schematic representation of the Atomic Force Microscopy single-cell force spectroscopy experimental setup: **a** The cantilever picks up a small amount of AB epoxy adhesive at the tip. **b** A single silica sphere is attached to the center of the cantilever to form the colloidal probe. **c** The probe is initially coated with polydopamine; subsequently, a single viable PSB cell attaches to the center of the sphere, visualized under a fluorescent microscope. **d** Force measurements are conducted between the colloidal probe and various biochar substrates in a liquid environment

Liftshitz-van der Waals interaction (LW), and ϕ_{bwp}^{EL} corresponds to the electrostatic double-layer interaction (EL), and ϕ_{bwp}^{AB} is the Lewis acid–base interaction (AB), where the subscript b denotes biochar, w indicates the 1 × PBS solution, and p represents PSB bacterial strains. The corresponding parameters and constants are presented in Table S1.

The XDLVO force model, adapted based on Thwala et al. (2013), compares bacteria-biochar interaction forces with AFM force-distance spectroscopy data, presenting outcomes in force (nN). Please refer to the Supporting Information (Text S6) for detailed computational methods.

2.8 Statistical analysis

Statistical analyses were conducted using IBM SPSS (Armonk, NY), with A univariate analysis of variance (ANOVA) and the Least Significant Difference (LSD) test assessing group differences, and Pearson's correlation coefficient examining variable correlations ($p < 0.05$ for significance). Principal Component Analysis (PCA) was performed on the physicochemical properties of biochar and bacterial adhesion data using Prism 9.0 (GraphPad Software, USA). This multivariate statistical technique reduced the dimensionality of the data and highlighted the most significant variables affecting the observed trends.

3 Results and discussion

3.1 Quantification of phosphate solubilization capacity, SEM imaging, and EPS analysis

To optimize inoculant performance, we compared the phosphate-solubilizing capacities of *A. pittii* and *B. subtilis* with *Bacillus megaterium*. In our previous study (Wang et al. 2022), we demonstrated the strong phosphate-solubilizing ability of *B. megaterium*, making it a suitable reference strain. Its well-characterized properties ensured a controlled and reliable comparison for evaluating the potential of *A. pittii* and *B. subtilis*. Additionally, *B. megaterium* is widely recognized for its phosphate-solubilizing capacity, further supporting its relevance as a benchmark in agricultural applications (Kang et al. 2014). The phosphate-solubilizing capabilities of *A. pittii* (194.85 mg L^{-1}) and *B. subtilis* (183.52 mg L^{-1}) surpassed that of *B. megaterium* (102.61 mg L^{-1}), as demonstrated over 5 days of cultivating, highlighting

the potential of both species as effective biochar-PSB soil inoculants (Fig. S1a). The enhanced phosphate-solubilizing efficacies of *A. pittii* and *B. subtilis* might originate from their increased secretion of organic acids, which solubilize phosphate, as evidenced by the substantially lower pH values observed in the respective Pikovskaya (PVK) media (Fig. S1b) (Zhu et al. 2018). Both species formed transparent halos of solubilized phosphate on PVK agar plates (Fig. S2).

SEM images revealed that *A. pittii* and *B. subtilis* formed biofilms on the surfaces and in pore spaces of biochar, produced at varying pyrolysis temperatures (Fig. 2). This observation suggests that despite differences in properties resulting from varying pyrolysis conditions, cotton straw-derived biochar effectively served as an effective carrier for these PSB species. As demonstrated in Fig. S3, large surface area and porous nature of biochar are conducive to bacterial attachment, growth, and biofilm formation. These properties enhance nutrient availability, bolster resilience against environmental challenges, and render biochar an ideal substrate for microbial growth (Mukherjee et al. 2022).

We further quantified the primary EPS constituents, polysaccharides and proteins. Cotton straw biochar

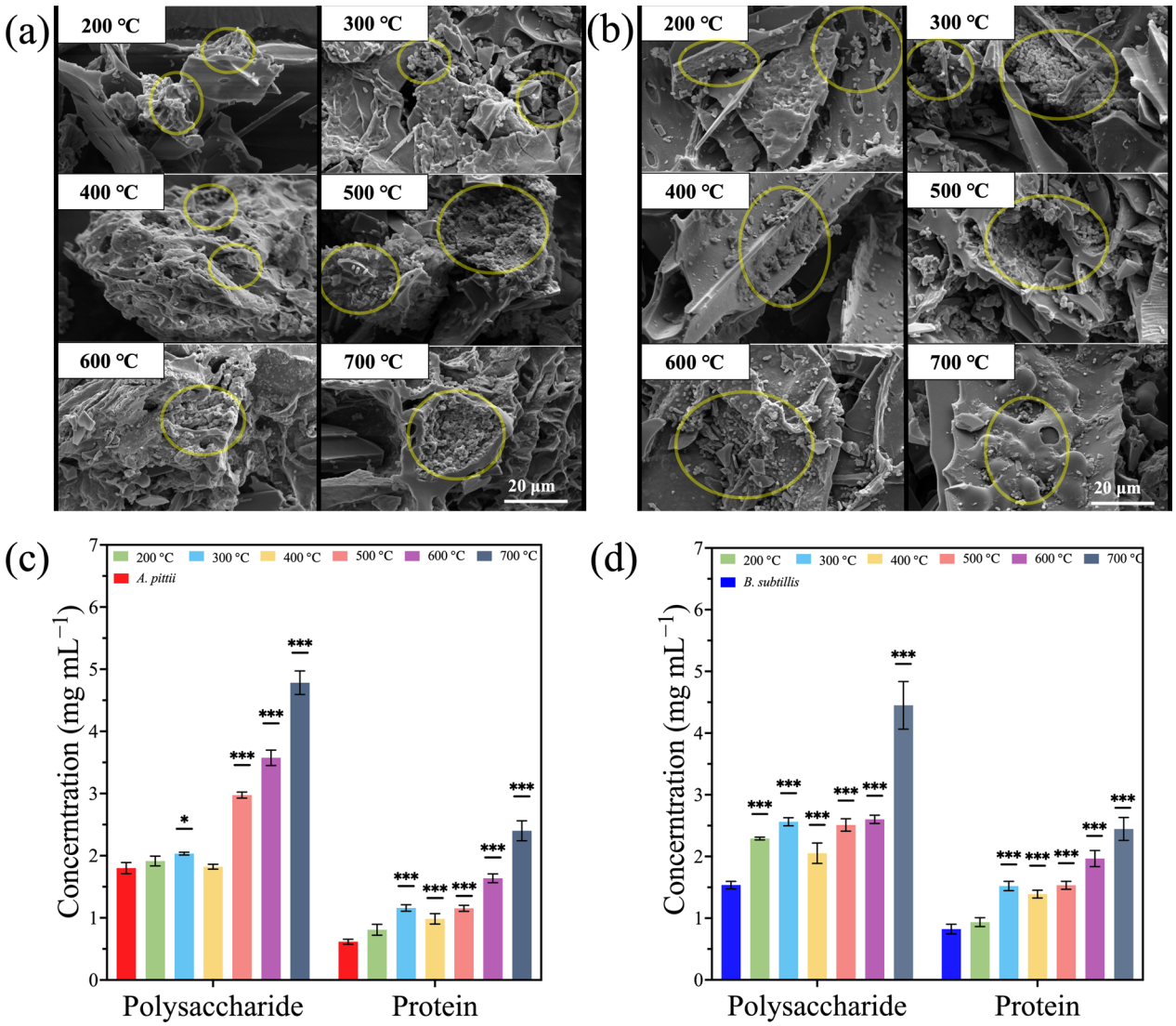

Fig. 2 SEM images of the presence of (**a**) *A. pittii* and (**b**) *B. subtillis* on biochar, with yellow circles indicating the locations of bacterial cells. Images are arranged by pyrolysis temperatures, ranging from 200 °C to 700 °C, corresponding to biochar samples CS200 through CS700. The respective concentrations of polysaccharide and protein components in the EPS for (**c**) *A. pittii*, and (**d**) *B. subtillis*. Asterisks indicate significant differences at $p < 0.05$ (***: $p \le 0.001$, **: $p \le 0.01$, *: $p \le 0.05$)

Table 1 Physicochemical properties of cotton biochar produced at temperatures ranging from 200 °C to 700 °C

Pyrolysis temperature (℃)	pH	EC (ds m^{-1})	WHC (%)	Hydrophobicity (°)	SA (m^2 g^{-1})	Pore size (nm)	TPVs (cm^3 g^{-1})	Yield (%)	Ash (%)	Elemental percentage (%)					Elemental ratio[a]			
										N	C	H	S	O	C/N	H/C	O/C	(O + N)/C
200	7.49 ± 0.025	2.325 ± 0.095	233.99 ± 4.45	77.7	4.38 ± 0.019	12.47 ± 0.073	0.0137	59.78%	8.23 ± 0.04	1.16	67.72	4.352	0.151	26.617	0.771	0.295	68.109	41.017
300	8.96 ± 0.171	4.14 ± 0.016	249.09 ± 13.21	72.1	6.09 ± 0.066	10.38 ± 0.066	0.0162	40.50%	8.85 ± 0.06	1.01	77.47	3.353	0.183	17.984	0.519	0.174	89.487	24.518
400	9.77 ± 0.047	4.323 ± 0.031	257.25 ± 7.51	48.8	7.91 ± 0.085	7.93 ± 0.112	0.0206	34.71%	10.12 ± 0.07	1.12	77.75	3.279	0.164	17.687	0.506	0.171	80.99	24.189
500	10.05 ± 0.04	5.798 ± 0.062	277.34 ± 4.25	42.7	15.54 ± 0.378	7.91 ± 0.068	0.0311	30.40%	11.43 ± 0.11	0.95	81.4	2.585	0.173	14.892	0.381	0.137	99.965	19.462
600	10.16 ± 0.044	8.37 ± 0.025	321.42 ± 13.64	35.9	27.40 ± 1.118	3 ± 0.028	0.0337	26.48%	12.69 ± 0.09	0.79	82.16	2.211	0.159	14.68	0.323	0.134	121.333	18.829
700	11.8 ± 0.01	9.675 ± 0.045	369.57 ± 10.08	24.1	79.63 ± 5.529	2.0238 ± 0.004	0.0404	26.05%	16.73 ± 0.08	1.19	83.72	1.339	0.165	13.586	0.192	0.122	82.078	17.649

[a] C/N, H/C, O/C, and (O + N)/C, are utilized to estimate the N availability (Lehmann et al. 2003), the level of carbonization, the surface's hydrophobicity, and the polarity of biochar (Al-Wabel et al. 2013)

The table includes *EC* Electric Conductivity, *WHC* Water Holding Capacity, *SA* BET-N_2 Surface Area, and *TPV* Total Pore Volume. Hydrophobicity is determined by the water contact angle, with a larger angle indicating increased surface hydrophobicity

generated under all pyrolysis temperatures increased the synthesis of both *A. pittii* and *B. subtilis* (Fig. 2c and d). Protein secretions for both strains were significantly enhanced at low pyrolysis temperatures, excluding CS200 ($p < 0.05$). Polysaccharide production in both strains showed a significant increase at all pyrolysis temperatures, except for CS200 and CS400 in the case of *A. pittii* ($p < 0.05$). Both PSB species secreted more EPS when immobilized on biochar compared to when cultured without it, especially pronounced for biochar produced at higher pyrolysis temperatures—specifically for *A. pittii* at CS600 and CS700, and *B. subtilis* at CS700. Results showed that biochars produced at higher pyrolysis temperatures significantly enhanced EPS production, likely due to the increased surface area and altered surface chemistry of the biochar, which make it more conducive to bacterial colonization. This phenomenon can be explained by the marked increase in EPS secretion, which acts as an adaptive mechanism employed by bacteria to better attach to and colonize biochar surfaces with these altered physicochemical properties. This is evident from our experimental results, which demonstrated a clear increase in EPS production at higher pyrolysis temperatures, particularly at 600 °C and 700 °C. This phenomenon corresponds with the research conducted by Guo et al. (2021), who noted that biochars processed at temperatures higher than 600 °C decrease bacterial transport, likely due to expanded surface areas and modified biochar properties. Such modified surfaces may encourage EPS secretion as a defensive mechanism against changes in surface chemistries (Table 1).

3.2 Characterization of biochar and PSB immobilization

In the immobilization of PSB using various biochars, the process initially plateaued on some biochars, including CS200 (Fig. S4). Unsurprisingly, increased bacterial concentrations enriched bacterial immobilization on biochar at all temperatures. This pattern suggests that at lower bacterial concentrations, PSB cells rapidly occupy the most accessible, high-affinity sites on the biochar (Bolan et al. 2023). Higher bacterial concentrations led to increased bacterial layering and aggregation. With increased bacterial inoculation dosages known to boost biofilm formation (Kragh et al. 2016), biochars pyrolyzed at higher temperatures (e.g., CS500, CS600, and CS700) have been observed to more effectively increase bacterial immobilization (Fig. S4). This increase is also associated with elevated levels of polysaccharides and proteins in the EPS, as demonstrated in Figs. 2c and d. At the highest bacterial concentrations, high-temperature biochar (e.g., CS500 and CS700) showed a robust capacity to host bacteria. Residual impurities in biochar (particularly low-temperature pyrolysis, e.g., CS200), such as volatile substances and partially carbonized matter, may originate from incomplete decomposition and impede bacterial immobilization (Tomczyk et al. 2020). Among the biochar samples (Fig. S4), CS400 showed relatively low immobilization of PSB, likely due to its specific physical and chemical properties. While surface area can support microbial retention, intermediate surface area at CS400 (7.91 $m^2\ g^{-1}$) alone may be insufficient, as effective immobilization also depends on micropore accessibility and surface chemistry (Mohanty et al. 2014). The mesoporous structure indicated by the pore size of CS400 (7.93 ± 0.112 nm) may be less favorable for microbial attachment compared to micropores, which offer protected niches for bacterial retention (Reddy et al. 2014). Additionally, a high pH at CS400 (9.77 ± 0.047) could limit PSB immobilization. Besides, electrostatic interactions by carboxyl and hydroxyl groups of biochars for microbial adherence may be limited at CS400 (Zhu et al. 2018). Interestingly, CS700 and CS600 showed a slight decrease in immobilization at peak bacterial dosages compared to CS500 (Fig. S4). The decrease in specific microporosity and pore size of biochar, which are crucial for bacterial adsorption, likely stems from changes in pore structure occurring at higher pyrolysis temperatures (Tomczyk et al. 2020). Guo et al. (2022) observed that biochar pyrolyzed at high temperatures, with larger surface areas and stronger adsorption capacities, can envelop bacteria, hindering the exchange of substances among cells and thus suppressing bacterial growth and reproduction. These results underline the complexity of the interactions between biochar properties and bacterial immobilization.

Fig. S5 shows the hydrophilic characteristics of the bacteria. The cell surface hydrophobicity values of *B. subtilis* and *A. pittii*, were 25.1% and 24.02%, demonstrating the hydrophilic natures of the two PSB species, indicating an affinity for polar substrates (Krasowska and Sigler 2014). The observed negative correlation between the hydrophilicity of biochar and its ζ-potential suggested complex interactions at the surface, potentially involving polar or ionizable groups (Fig. S6a, S7b and S7c). The adhesion of hydrophilic bacteria such as *B. subtilis* and *A. pittii*, which display negative surface charges, to biochar surfaces may be influenced by both charge interactions and the specific surface characteristics of the biochar.

3.3 Analysis and interpretation of FTIR spectra

Figure 3 compares the FTIR spectra of *A. pittii* and *B. subtilis* immobilized biochar to pristine biochar, revealing vital functional groups for microbial adhesion. The spectra demonstrated pronounced hydroxyl (–OH) stretching vibrations at approximately 3400 cm^{-1} across all biochar

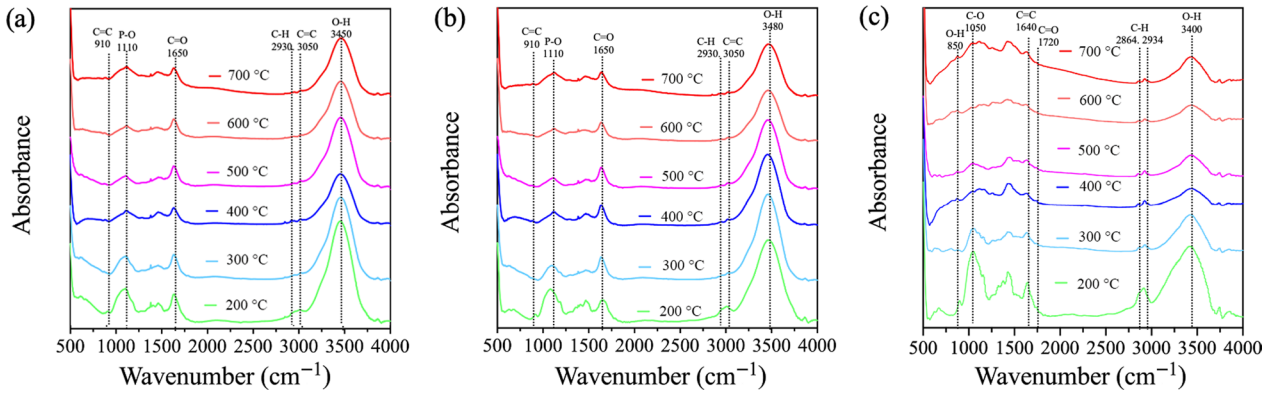

Fig. 3 FTIR spectra comparisons of (a) biochar immobilized with *A. pittii*, (b) biochar with *B. subtilis*, and (c) pristine biochar

samples immobilized with each PSB strain. The intensities of these vibrations were notably higher in biochar samples pyrolyzed at 400, 500, 600, and 700 °C compared to pristine biochar, indicating robust biochar–bacteria interactions. This enhancement in intensity likely reflects increased functionalization or structural adaptations in biochar surfaces that facilitate stronger microbial adherence at these specific pyrolysis temperatures (Huang et al. 2023; Qu et al. 2022). This was complemented by the presence of amide I bands at 1650 cm^{-1}, constituent proteins within EPS that likely contribute to robust biochar–bacteria connections and potential biofilm formation. P–O stretching vibrations around 1100 cm^{-1} were attributed to phosphorus groups on biochar, as PSB interact with nutrient reservoirs to modulate phosphorus release or storage (Liu et al. 2023). Alterations in the C=O stretching peak around 1720 cm^{-1} pointed to modifications in the carboxylic acid groups, which upon deprotonation into carboxylate anions (–COO^{-}), may augment bacterial adhesion by providing additional sites for electrostatic interaction (Biniak et al. 2016).

The FTIR analysis also clarified the enrichment of oxygen-containing functional groups, particularly in biochar pyrolyzed at 200 and 300 °C, despite its reduced surface area limiting PSB immobilization (Fig. S4). This is consistent with the findings by Liu et al. (2018), which demonstrated the role of pyrolysis at 200 and 300 °C in preserving high levels of functional groups, thereby enhancing the adsorption capabilities and chemical stability of biochar. This demonstrates that biochar produced at lower temperatures, like CS300, maintains an immobilization efficacy comparable to that of biochar produced at higher temperatures, such as CS600, substantiating the potential of varied biochar substrates in microbial adhesion and biofilm development processes (Huang et al. 2023).

3.4 Insights into PSB–biochar interactions using SCFS measurements

The adhesion force patterns in Fig. 4a and b illuminate the strength of immediate post-contact adhesive interactions, providing quantitative insights into how PSB engage with biochar surfaces at the nanoscale during the reversible adhesion phase. The adhesion of *A. pittii* and *B. subtilis* onto biochar demonstrated complex, nonlinear responses to variations in pyrolysis temperature. *B. subtilis* showed a steady adhesion force with CS200 (1.778 nN), which escalated to 3.280 nN with CS300 and peaked at 4.409 nN with CS700. *A. pittii* demonstrated stable forces of 2.546–2.844 nN with CS200, CS400, and CS600, higher forces with CS300 and CS500, and a peak at 4.147 nN with CS700. Our measured values align with the strong microbial adhesion interval described by Viljoen et al. (2020), particularly in contexts where bacteria interacted with surfaces that influence their attachment strategies. Moreover, the notable increase in atomic force at CS300 during the interaction between both PSB strains and biochar is an intriguing phenomenon. This effect can be attributed to the retention of surface functional groups and the optimal balance of chemical properties at this intermediate pyrolysis temperature for enhanced bacterial adhesion.

Fig. S8 shows the representative adhesion-distance curves for bacterial–surface interactions. The results indicate that variations in the strengths of bacterial–surface interactions during the reversible adhesion phase are influenced by the distinct characteristics of biochar surfaces produced at different pyrolysis temperatures. These variations likely stem from a combination of specific and nonspecific forces, including hydrogen bonding and steric hindrance, which were reflected in the differences observed in our experimental data. Specifically, our adhesion-distance curves indicate that higher pyrolysis

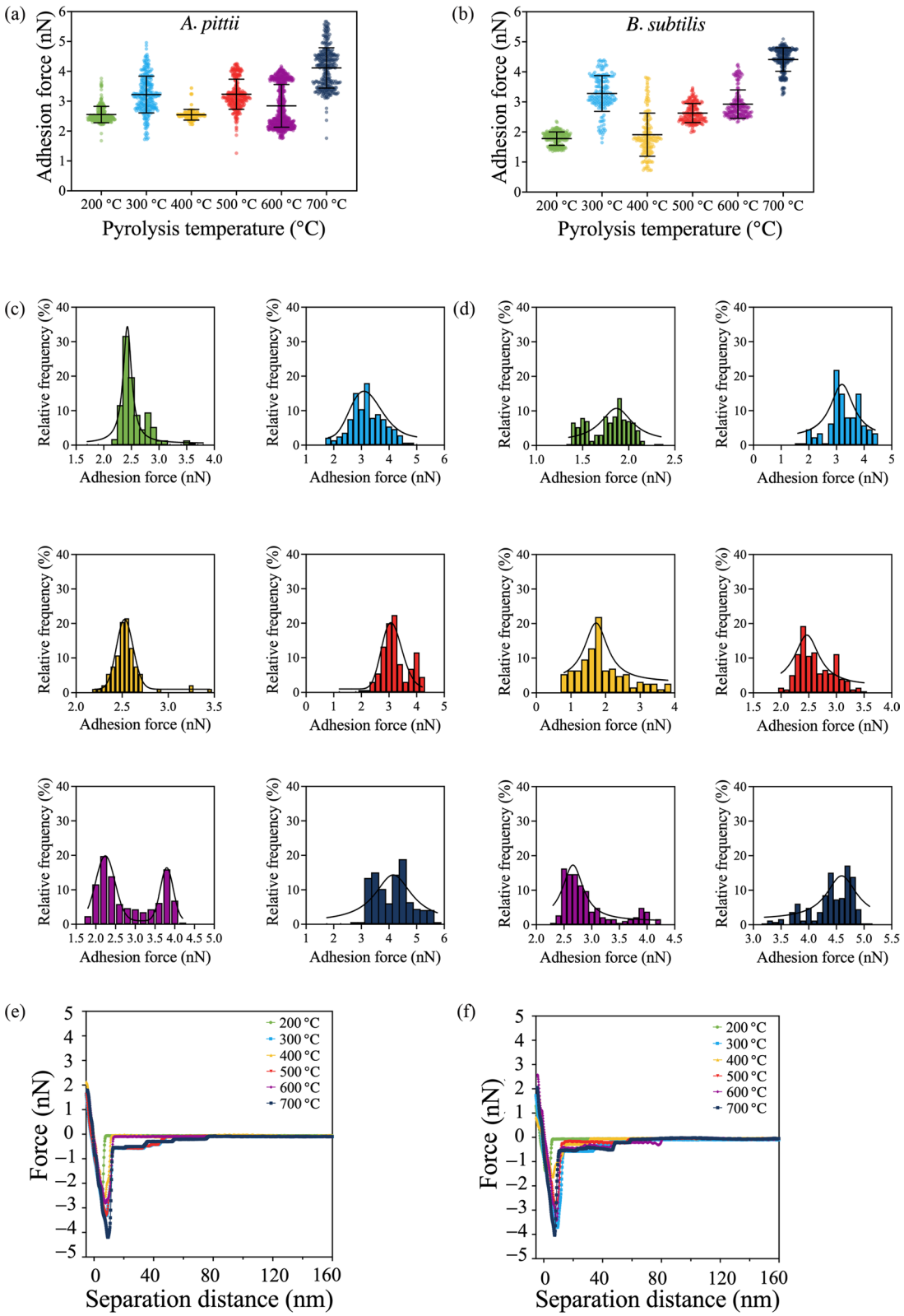

Fig. 4 AFM adhesion forces for *A. pittii* (**a**, n ≥ 200) and *B. subtilis* (**b**, n ≥ 200) subjected to various biochar as substrate immersed in aquatic environment. Histograms of adhesion force, fitted with Gaussian distribution, are presented for (**c**) *A. pittii*, and (**d**) *B. subtilis*. Representative approach force-distance curves are shown for (**e**) *A. pittii and* (**f**) *B. subtilis*

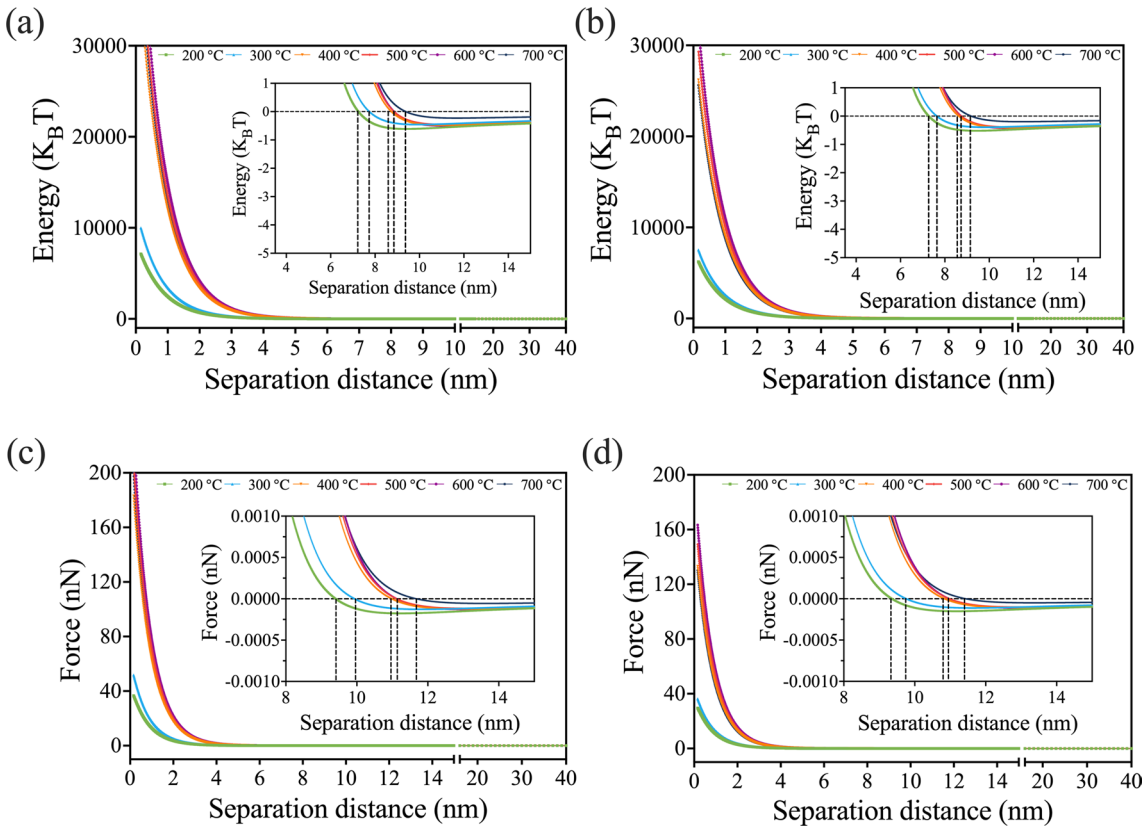

Fig. 5 XDLVO predictions for different bacteria strains interacting with various biochar. Energy profiles for (**a**) *A. pittii* and (**b**) *B. subtilis* are presented in units of K_BT. Force profiles for (**c**) *A. pittii* and (**d**) *B. subtilis* are presented in nanonewtons (nN). Dotted lines represent where $\phi^{Total} = 0$ or $F^{Total} = 0$ for (**a**) (**b**) and (**c**) (**d**)

temperatures enhance surface complexity, which appears to promote stronger adhesion through these forces. These findings are supported by the observations of Berne et al. (2018), who indicated that hydrogen bonding can initiate bacterial adhesion. Additionally, Martínez et al. (2018) highlighted that the altered surface area, chemical functionality, and physicochemical properties of biochar, induced by different pyrolysis temperatures, can affect bacterial interactions. Collectively, these studies illustrated that microbial adhesion to biochar is influenced by both microbial characteristics and the evolving properties of biochar, which is essential for optimizing its use in environmental and biotechnological applications. The asymmetric distribution observed in the frequency histogram suggested the heterogeneous natures of both the biochar surface and the bacterial cell surfaces (Fig. 4c and d) (Dorobantu et al. 2008). Meanwhile, snap-in events noted during the approach phase of AFM probes confirmed the presence of pre-contact attraction forces (Fig. 4e and f) (Olubowale et al. 2021). The findings imply the existence of other complex mechanisms beyond simplistic linear models and straightforward data interpretation. We next applied the XDLVO theory, in conjunction with AFM, to yield a comprehensive understanding of the mechanisms involved.

3.5 Comparative analysis of XDLVO theory and interacting force measurements for interfacial dynamics

At large distances, neither the XDLVO models nor AFM approach curves revealed biochar–bacteria interactions (Fig. 4e, f and 5). The absence of interactions at such large distances indicates the potential necessity for an externally driven force or mechanism to first place PSB in the proximity of PSB to the biochar surface. As PSB neared the biochar surface, the theoretical XDLVO model curves displayed a shift in energy from positive (repulsion) to negative (attraction) (Fig. 5a and b). This shift suggested a secondary minimum, a state in which bacterial cells are trapped by weak attraction but remain vulnerable to external disturbances (Berne et al. 2018). Similarly, in Fig. 4e and f, the AFM approach curves substantiated this prediction. For *A. pittii* interacting with CS200 to

CS700, the secondary minimum depths were − 0.61, − 0.45, − 0.48, − 0.45, − 0.50, and − 0.23 K_BT; for *B. subtilis*, the respective depths were − 0.52, − 0.39, − 0.41, − 0.39, − 0.43, and − 0.20 K_BT. Our findings indicate that the secondary minimum depths for *A. pittii* and *B. subtilis* exhibited variability across different pyrolysis temperatures, with a notable reduction observed at CS700, suggesting that biochar produced at higher temperatures alters the adhesion profile by weakening the attractive forces between bacterial cells and biochar. This result is consistent with the findings by Ruan et al. (2020), which demonstrated that the adhesion of *Sphingomonas* sp. to montmorillonite was governed by long-range XDLVO forces, such as electrostatic and van der Waals interactions, in environments with lower ionic strength. To align the theoretical predictions of the XDLVO model with the experimental force − distance measurements obtained from AFM, the energy profiles have been translated into force profiles for a more straightforward comparison of the interactions.

The XDLVO force profiles (Fig. 5c and d) revealed shallow attraction within the secondary minimum, attributed solely to LW forces. This was particularly notable given that EL interactions led to mutual repulsion resulting from surface charges of the same polarity (Fig. S7); AB interactions were similarly repulsive, with $\Delta G^{AB} > 0$ (Table S2). This phenomenon is attributed to attractive forces, primarily governed by a Hamaker constant calculated within the XDLVO framework (approximately 10^{-22} J m^{-2}) (Table S3). Our results fell within the lower range of reported values but aligned with studies conducted by Matsumoto et al. (2012) and Brown and Jaffé (2006), who demonstrated that bacteria could interact with solid substrates across water. The predicted attractive forces differed notably, 4–5 orders of magnitude lower than the values obtained from the AFM approach curves (Fig. 4e, f, and 5). The model showed that CS200 possessed the greatest potential for attraction with both PSB species, diverging from the AFM results. These disparities point to a complex interplay of forces, not only van der Waals forces but also forces relating to hydrodynamic (Alam et al. 2019), steric effects (Hwang et al. 2018), and bacterial surface proteins (Olubowale et al. 2021), all crucial in bacterial cell attraction. Our results also demonstrate that surface properties and hydrodynamic conditions, such as wetting, significantly influence adhesion dynamics. It highlights the involvement of multiple forces in shaping bacterial behavior on biochar surfaces. This finding is consistent with previous research (Mu et al. 2023), which indicates that such interactions are influenced by various factors beyond traditional attractive forces. These interactions suggested limitations in the explanatory power of the XDLVO theory for such complex phenomena.

When the separation distance surpassed the secondary minimum and approached the equilibrium cut-off point, the intensifying overlap of electrical double-layers, coupled with repulsive acid–base interactions, led to substantially stronger repulsion. Simultaneously, as previously noted, LW forces contributed to a weak attraction. Together, these factors established high-energy barriers that obstructed the final contact of bacteria and biochar (Fig. 5a and b). The lowest predicted energy barriers, 7133.77 K_BT (36.64 nN) for *A. pittii* and 6238.77 K_BT (29.53 nN) for *B. subtilis*, were observed when they interacted with the CS200. These predictions were notable compared with the attraction from LW forces or the attractive forces observed in the approach curves. Significant primary energy barriers inhibiting bacterial adhesion to biochar surfaces were observed, particularly at CS200. It can be concluded that dynamic changes in interfacial energy and energy barriers play a crucial role in shaping adhesion behavior. Similarly, Song et al. (2021) demonstrated that dynamic interfacial changes can influence energy barriers at microbial interfaces over time, thereby increasing the susceptibility of surfaces to bacterial adhesion and subsequent biofouling. Similarly, biochar immersed in a liquid environment likely exhibits comparable behaviors, with shifts in interfacial energies affecting microbial adhesion. This highlights the importance of considering these dynamics when studying microbial interactions with substrates. It is essential to note that the approach of the AFM probe, driven by a preset force setpoint, acts as an external force to surmount this substantial primary energy barrier. Under natural conditions, an externally driven force would be absent. The use of 1 × PBS buffer to simulate inoculant conditions in this study compressed the electrostatic interactions between bacteria and biochar due to the increased ionic strength (Shafiei-Sabet et al. 2014). The effective surface potential (Ψ) diminishes significantly with increasing separation distance (Schwegmann et al. 2013). This dynamic process facilitates the closer approach of PSB to biochar. Despite the favorable parameters in the XDLVO model that showed lower energy barriers via attenuated repulsion, the barriers remained too high for bacteria to establish contact.

The observed discrepancies between XDLVO theoretical modeling and adhesion force measurements, evident when compared to the SEM imagery and actual bacterial immobilization outcomes, might stem from aspects inadequately captured by current theoretical models and experimental approaches. For instance, surface proteins secreted by various bacterial species, known as adhesins, are crucial for initiating contact (Le Guennec et al. 2020), a complexity underscoring

the limits of the XDLVO theory in explaining microbial interactions. Furthermore, XDLVO theory is based on assumptions of idealized and smooth surfaces, and therefore does not account for the inherent heterogeneity and roughness of actual biochar surfaces. These surface complexities, including variations in texture, porosity, and functional groups, can significantly influence microbial adhesion but present challenges for accurate incorporation into theoretical models. On the other hand, the SCFS method concentrates on single-cell level interactions and may not fully reflect the behaviors of entire bacterial populations. The adhesion force outcomes distinctly demonstrated the variations between gram-positive and gram-negative bacteria, and it is important to acknowledge that the force measurements obtained may have been affected by the distinct elasticity and deformability characteristics inherent to the different cell wall compositions of these bacteria (Weidenmaier and Peschel 2008). The high sensitivity of AFM to experimental conditions can contribute to inconsistencies in results, particularly when using the SCFS method. This issue is compounded by variability in the properties of bacterial cells and biochar surfaces, as well as challenges in maintaining uniform cell orientations. Mohamed Zuki et al. (2021) further highlighted that the orientation of cells itself can significantly influence adhesion outcomes. The complex interactions and discrepancies revealed by AFM and XDLVO theory highlight the need to integrate theoretical models with experimental validations to understand interfacial dynamics comprehensively.

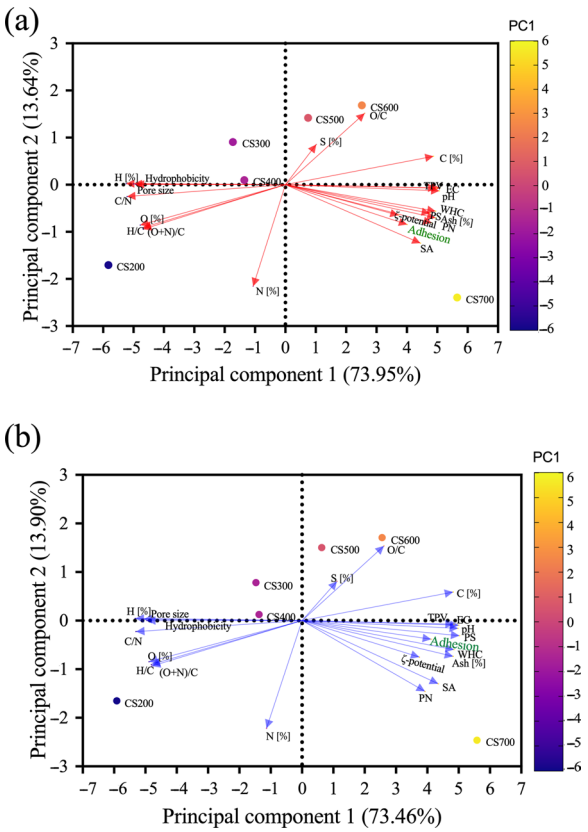

Fig. 6 PCA illustrating the relationship between physicochemical properties of biochar and EPS components polysaccharide (PS), and protein (PN), in association with bacterial adhesion for (**a**) *A. pittii* and (**b**) *B. subtilis*

3.6 Distinguishing factors influencing PSB adhesion

Bacterial adhesion onto biochar is driven by complex physicochemical and biological interactions, which we investigated via principal component analysis (PCA). Figure 6 presents the PCA plots, in which coloured dots denote the biochar types, and the associated physicochemical properties and biofilm components are represented by corresponding colored arrows. For both *A. pittii* and *B. subtilis*, the first two PCs captured over 87% of the variance. Polysaccharide and protein concentrations, alongside various physicochemical attributes of biochar (e.g., surface area, electrical conductivity, ζ-potential, water holding capacity, and ash content), were positively associated with PSB adhesion (Table S4). Notably, the initial reversible adhesion showed a positive correlation with polysaccharide and protein concentrations, exhibiting R^2 values of 0.727 and 0.671 for *A. pittii*, and 0.765 and 0.712 for *B. subtilis*, respectively. As Limoli et al. (2015) highlighted, increased polysaccharide and protein contents can assist PSB immobilization and robust biofilm matrix formation. Feng et al. (2021) also noted that bioactive polysaccharides play pivotal roles in various physiological processes, including cell recognition, metabolism, and immune responses. Strong reversible adhesion enhances biofilm stability, benefiting bacteria by securing essential components like polysaccharides and proteins, which in turn prevent detachment and maintain the integrity of the biofilm. Larger surface areas offer more space for bacterial immobilization, and greater pore volumes provide more environmental protection (Sun et al. 2016). Biochar with higher electrical conductivity possesses a denser distribution of charged sites, which intensifies electrostatic attraction and augments ion exchange capacity, fostering an environment conducive to bacterial attachment (Li et al. 2018). Meanwhile, enhanced water-holding capacity (WHC) of biochar contributes significantly to water retention, creating a more hydrated environment. This not only supports bacterial activity and promotes their spontaneous motion and adhesion but also plays a crucial role in impeding runoff, highlighting the multifaceted benefits of biochar in soil management (Li et al. 2008). As already mentioned, a less negative ζ-potential on the biochar surface

can reduce repulsion, enhancing adhesion. In addition, biochar with higher ash contents may serve as a nutrient reservoir, supporting PSB growth and activity by supplying essential inorganic minerals and elements (Bolan et al. 2023). Physicochemical properties of biochar significantly influence bacterial adhesion and biofilm formation. To refine biochar for practical use, methods such as physical activation with steam or acid–base treatments and using mineral-rich biomass as feedstock can be applied (Wang and Wang 2019). These tailored modifications aim to optimize performance of biochar for specific applications while promoting ecological sustainability and environmental health.

Caution is warranted when interpreting PCA results, as this analytical method can collectively categorize variables as positive influencers on bacterial adhesion, even when individual factors may have contrasting effects. For instance, CS700 had a high pH value of 11.8, in contrast with the preference of bacteria for environments with natural (pH = 7) (Zheng et al. 2019). Key negative influencers were also identified, such as surface hydrophobicity, nitrogen availability, the degree of carbonization, and surface polarity.

3.7 PSB-biochar immobilization mechanism

Focusing solely on PSB adhesion forces provides valuable insights, and such an approach may oversimplify the complexity inherent in such interactions. For instance, at the secondary minimum, observed discrepancies between force measurements and model predictions called for analyzing these attractions, incorporating both modeled forces and other interactions, to thoroughly understand the approach of PSB to biochar. By synthesizing the experimental observations with the modeling results, we proposed a mechanism to elucidate this interfacial dynamic process (Fig. 7).

At large separation distances, planktonic bacteria were subject to gravitational forces, mechanical mixing,

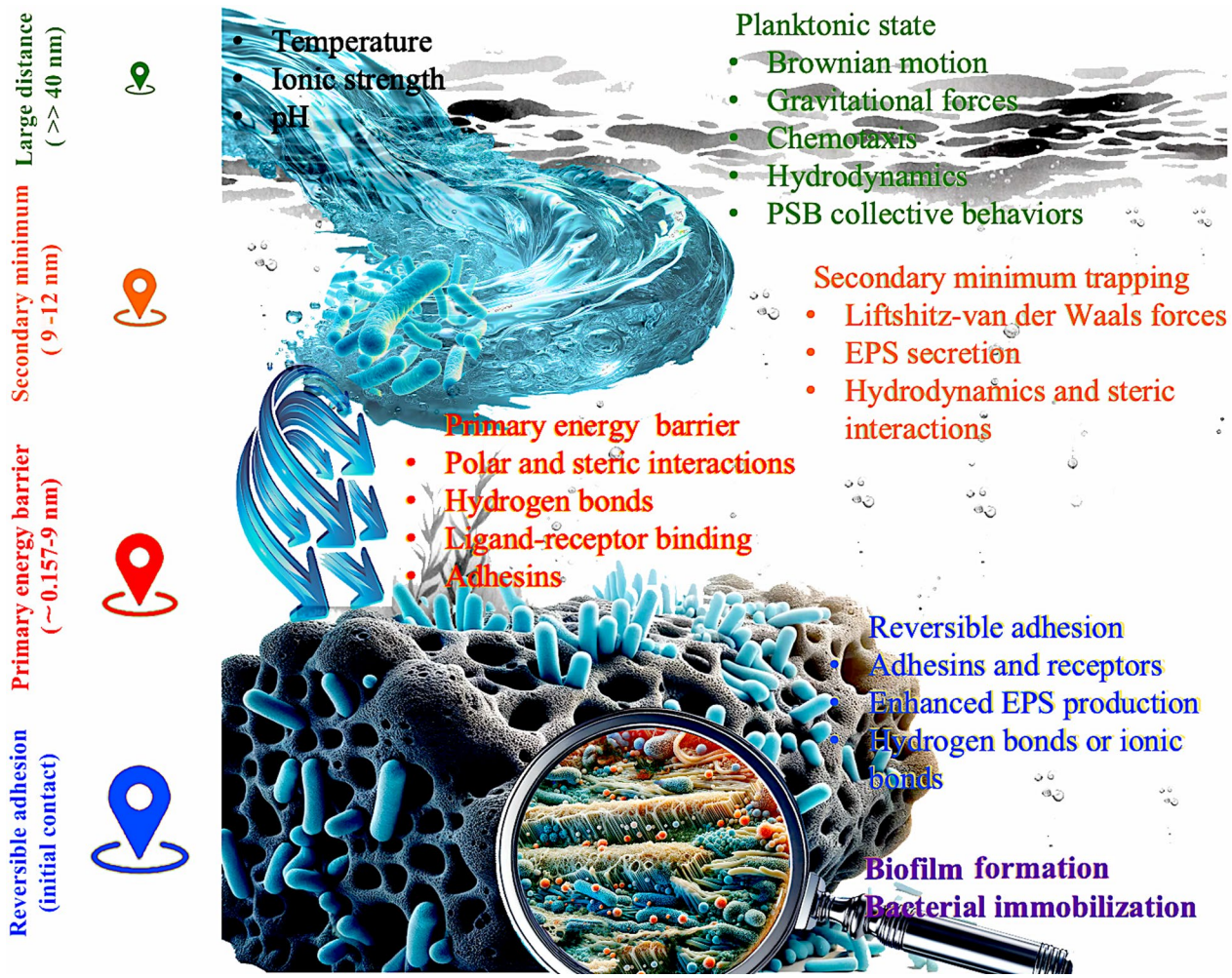

Fig. 7 Schematic representation of the potential mechanisms for the immobilization of PSB onto cotton straw-derived biochar surfaces

chemotaxis, and inherent movements such as Brownian motion (Berne et al. 2018), as well as bacterial population behaviors (Li et al. 2008). Fluid dynamics significantly influenced cell movement toward biochar in soil inoculant preparations, and this effect was further augmented by the collective behavior of densely inoculated bacterial populations (Lushi et al. 2014). These combined dynamics synergistically promoted bacterial proximity to biochar surfaces in aqueous environments. Approaching the secondary minimum, a discernible attraction was present, as previously mentioned. This, coupled with steric interactions and the EPS secretion (Liu et al. 2010), effectively trapped the PSB, facilitating their approach toward the biochar. Extending beyond the secondary minimum, numerous factors played crucial roles in overcoming the realm of the primary energy barrier. These include bacterial motility, polar interactions (Krsmanovic et al. 2021), and steric interactions (Feng et al. 2015), along with surface interactions like hydrogen bonds and ligand-receptor binding at close proximity (Carniello et al. 2018; Chen et al. 2016). In conjunction with the diverse expression of adhesins on the bacterial cell surface, these factors collectively empowered bacteria to surmount the substantial energy barrier.

Gram-positive bacteria like *B. subtilis* use proteinaceous adhesins for specific surface interactions, whereas gram-negative bacteria like *A. pittii* have a lipopolysaccharide-rich outer membrane that harbors adhesins and appendages like pili or fimbriae (Chai et al. 2021). Ultimately, the process, aided by ionic and hydrogen bonding (Chen et al. 2016), culminated in the reversible adhesion of PSB to biochar. The strength of the reversible adhesion between PSB and biochar aided in resisting external disturbances under dynamic environmental conditions, supporting the initiation of biofilm matrix formation and bacterial immobilization. It is noteworthy that factors such as temperature, ionic strength, and pH of the surrounding aqueous environment critically influenced the dynamics of this process. Moderate temperatures within the inoculant conditions create favorable environments for microbial growth and stable adhesion on biochar surfaces by enhancing bacterial metabolic activity and adhesion stability (Zeng et al. 2023). Similarly, ionic strength in the inoculant conditions can be adjusted to modulate electrostatic interactions between biochar and microbial cells: increased ionic strength generally reduces repulsive forces, thereby promoting adhesion, though excessively high ionic strength may impair cell function (Uchimiya 2014). Additionally, pH influences the charge on both biochar surfaces and microbial cell walls with neutral to slightly acidic pH conditions generally favoring microbial attachment (Hamadi et al. 2004). Consequently, while high-temperature biochar, such as CS700, demonstrates the highest immobilization rate of PSB and strong adhesion forces, its elevated pH presents challenges for soil application. To address this, practical modifications—such as acid washing, incorporation of acidic amendments, or CO_2 treatment—can be applied to reduce its pH. These adjustments would enhance soil compatibility while retaining structural stability of biochar and effectiveness as a long-term inoculant carrier.

4 Conclusion

This study employed SCFS and AFM, combined with theoretical XDLVO modeling, to elucidate the immobilization mechanisms of two PSBs, *A. pittii* and *B. subtilis*, on biochar surfaces. Our findings reveal a significant correlation between the initial adhesion forces measured and subsequent biofilm formation, underscoring the importance of these forces in resisting detachment. Key physicochemical properties of cotton-straw derived biochar, such as larger surface area, higher water holding capacity (WHC), less negative ζ-potential, increased ash content, and higher electrical conductivity (EC), enhance PSB immobilization. A larger surface area provides adhesion sites, while high WHC maintains moisture, essential for bacterial metabolism. A less negative ζ-potential reduces repulsion with PSB cells, enhancing attachment to the biochar matrix. Increased ash content offers nutrients, and higher EC boosts nutrient exchange, supporting PSB viability and immobilization. Strategic modifications to the properties of PSB-biochar inoculants could enhance their effectiveness as carriers for PSBs in practical applications. We proposed a schematic immobilization mechanism that includes the following phases: planktonic interaction of PSBs, secondary minimum entrapment by attraction forces, primary barrier transcendence through multifactorial synergy, and initial reversible adherence, all of which collectively facilitate biofilm formation. Our results suggest that improving biochar-based inoculants for PSB immobilization enhances soil phosphorus availability. In future research, it is worthwhile examining how environmental factors such as plant interactions, soil composition, and water flow affect biochar–bacteria interface dynamics. Investigating a broader range of microorganisms, particularly those involved in nutrient cycling or heavy metal immobilization, could reveal diverse bacterial responses to biochar under natural conditions. Additionally, assessing the shelf life, biological activity, and long-term ecological impact of biochar-PSB inoculants will enhance our understanding of the role

of biochar as a sustainable inoculant carrier in various agricultural settings.

Abbreviations

PSB	Phosphate-solubilizing bacteria
CS	Cotton straw biochar
XDLVO	Extended Derjaguin-Landau-Verwey-Overbeek theory
AFM	Atomic force microscopy
SCFS	Single-cell force spectroscopy
EPS	Extracellular polymeric substances
CFU	Colony-forming units
PN	Protein
PS	Polysaccharide
SA	Surface area
WHC	Water holding capacity
TPV	Total pore volume
EC	Electric conductivity
LW	Lifshitz-van der Waals
EL	Electrostatic double-layer
AB	Lewis acid–base

Supplementary Information

The online version contains supplementary material available at https://doi.org/10.1007/s42773-025-00444-4.

Additional file 1.

Acknowledgements
The authors thank the support from Memorial University of Newfoundland.

Author contributions
Conceptualization: Bing Chen, Yiqi Cao, Baiyu Zhang, Shuguang Wang; Methodology: Zhe Wang, Sufang Xing; Formal analysis and investigation: Zhe Wang; Writing—original draft preparation: Zhe Wang; Writing—review and editing: Bing Chen, Yiqi Cao, Baiyu Zhang, Shuguang Wang, Huifang Tian; Funding acquisition: Bing Chen, Huifang Tian, Shuguang Wang; Resources: Bing Chen, Baiyu Zhang, Huifang Tian, Shuguang Wang; Supervision: Bing Chen, Baiyu Zhang, Huifang Tian, Shuguang Wang.

Funding
This work was supported by the National Natural Science Foundation of China (Grant No. 52200198), Taishan Scholars Project of Shandong Province (NO. tstp20230604), Natural Science Foundation of Shandong Province (Grant No. ZR2021QB186).

Availability of data and materials
All data generated or analyzed during this study are included in this published article. The datasets used or analyzed during the current study are available from the corresponding author on reasonable request.

Declarations

Competing interests
The authors declare that they have no known financial or non-financial conflicts of interest, either directly or indirectly related to the submitted work.

Author details
[1]Shandong Key Laboratory of Water Pollution Control and Resource Reuse, School of Environmental Science and Engineering, Shandong University, Qingdao 266237, China. [2]Northern Region Persistent Organic Pollution Control (NRPOP) Laboratory, Faculty of Engineering and Applied Science, Memorial University of Newfoundland, St. John's, NL A1B 3X5, Canada. [3]Sino-French Research Institute for Ecology and Environment (ISFREE), School of Environmental Science and Engineering, Shandong University, Qingdao 266237, Shandong, China. [4]Weihai Research Institute of Industrial Technology of Shandong University, Weihai 264209, China.

Received: 17 August 2024 Revised: 3 February 2025 Accepted: 6 February 2025
Published online: 13 March 2025

References

Adam J, Del Sorbo MR, Kaur J, Romano R, Singh M, Valadan M, Altucci C (2023) Surface interactions studies of novel two-dimensional molybdenum disulfide with gram-negative and gram-positive bacteria. Anal Lett 56(2):357–371
Ahmed MB, Zhou JL, Ngo HH, Guo W (2016) Insight into biochar properties and its cost analysis. Biomass Bioenergy 84:76–86
Alam F, Kumar S, Varadarajan KM (2019) Quantification of adhesion force of bacteria on the surface of biomaterials: techniques and assays. ACS Biomater Sci Eng 5(5):2093–2110
Al-Wabel MI, Al-Omran A, El-Naggar AH, Nadeem M, Usman AR (2013) Pyrolysis temperature induced changes in characteristics and chemical composition of biochar produced from conocarpus wastes. Bioresour Technol 131:374–379
Beaussart A, El-Kirat-Chatel S, Sullan RM, Alsteens D, Herman P, Derclaye S, Dufrene YF (2014) Quantifying the forces guiding microbial cell adhesion using single-cell force spectroscopy. Nat Protoc 9(5):1049–1055
Berne C, Ellison CK, Ducret A, Brun YV (2018) Bacterial adhesion at the single-cell level. Nat Rev Microbiol 16(10):616–627
Biniak S, Trykowski G, Walczyk M, Richert M (2016) Thermo-chemical modification of low-dimensional carbons: an infrared study. J Appl Spectrosc 83:580–585
Bolan S, Hou D, Wang L, Hale L, Egamberdieva D, Tammeorg P, Li R, Wang B, Xu J, Wang T (2023) The potential of biochar as a microbial carrier for agricultural and environmental applications. Sci Total Environ 886:163968
Brown DG, Jaffé PR (2006) Effects of nonionic surfactants on the cell surface hydrophobicity and apparent Hamaker constant of a Sphingomonas sp. Environ Sci Technol 40(1):195–201
Carniello V, Peterson BW, van der Mei HC, Busscher HJ (2018) Physico-chemistry from initial bacterial adhesion to surface-programmed biofilm growth. Adv Colloid Interface Sci 261:1–14
Chai WS, Cheun JY, Kumar PS, Mubashir M, Majeed Z, Banat F, Ho S-H, Show PL (2021) A review on conventional and novel materials towards heavy metal adsorption in wastewater treatment application. J Clean Prod 296:126589
Chai YN, Futrell S, Schachtman DP (2022) Assessment of bacterial inoculant delivery methods for cereal crops. Front Microbiol 13:791110
Chen D, Oezguen N, Urvil P, Ferguson C, Dann SM, Savidge TC (2016) Regulation of protein-ligand binding affinity by hydrogen bond pairing. Sci Adv 2(3):e1501240
Costa F, Carvalho IF, Montelaro RC, Gomes P, Martins MCL (2011) Covalent immobilization of antimicrobial peptides (AMPs) onto biomaterial surfaces. Acta Biomater 7(4):1431–1440
Das SK (2024) Adsorption and desorption capacity of different metals influenced by biomass derived biochar. Environ Syst Res 13(1):5
Dorobantu LS, Bhattacharjee S, Foght JM, Gray MR (2008) Atomic force microscopy measurement of heterogeneity in bacterial surface hydrophobicity. Langmuir 24(9):4944–4951
Eskhan A, Johnson D (2022) Microscale characterization of abiotic surfaces and prediction of their biofouling/anti-biofouling potential using the AFM colloidal probe technique. Adv Colloid Interface Sci 310:102796
Feng G, Cheng Y, Wang S-Y, Borca-Tasciuc DA, Worobo RW, Moraru CI (2015) Bacterial attachment and biofilm formation on surfaces are reduced by small-diameter nanoscale pores: how small is small enough? Npj Biofilms Microbiomes 1(1):1–9
Feng T, Yang X, Kong Q, Lu J (2021) Food bioactive polysaccharides and their health functions. Front Nutr 8:746255
Gaudy A (1962) Colorimetric determination of protein and carbohydrate. Ind Water Wastes 7:17–22
Głodowska M, Schwinghamer T, Husk B, Smith D (2017) Biochar based inoculants improve soybean growth and nodulation. Agric Sci 8(9):1048–1064
Guo S, Liu X, Zhao H, Wang L, Tang J (2021) High pyrolysis temperature biochar reduced the transport of petroleum degradation bacteria Corynebacterium variabile HRJ4 in porous media. J Environ Sci 100:228–239

Guo S, Liu X, Wang L, Liu Q, Xia C, Tang J (2022) Ball-milled biochar can act as a preferable biocompatibility material to enhance phenanthrene degradation by stimulating bacterial metabolism. Bioresour Technol 350:126901
Hamadi F, Latrache H, El Ghmari A, Ellouali M, Mabrrouki M, Kouider N (2004) Effect of pH and ionic strength on hydrophobicity and electron donor and acceptor characteristics of Escherichia coli and Staphylococcus aureus. Ann Microbiol 54:213–226
Hamaker HC (1937) The London—van der Waals attraction between spherical particles. Physica 4(10):1058–1072
Hartmann M, Six J (2023) Soil structure and microbiome functions in agroecosystems. Nat Rev Earth Environ 4(1):4–18
Huang J, Tan X, Ali I, Duan Z, Naz I, Cao J, Ruan Y, Wang Y (2023) More effective application of biochar-based immobilization technology in the environment: understanding the role of biochar. Sci Total Environ 872:162021
Hwang G, Gomez-Flores A, Bradford SA, Choi S, Jo E, Kim SB, Tong M, Kim H (2018) Analysis of stability behavior of carbon black nanoparticles in ecotoxicological media: hydrophobic and steric effects. Colloids Surf a: Physicochem Eng Asp 554:306–316
Kang S-M, Radhakrishnan R, You Y-H, Joo G-J, Lee I-J, Lee K-E, Kim J-H (2014) Phosphate solubilizing Bacillus megaterium mj1212 regulates endogenous plant carbohydrates and amino acids contents to promote mustard plant growth. Indian J Microbiol 54:427–433
Kragh KN, Hutchison JB, Melaugh G, Rodesney C, Roberts AE, Irie Y, Jensen PØ, Diggle SP, Allen RJ, Gordon V (2016) Role of multicellular aggregates in biofilm formation. Mbio
Krasowska A, Sigler K (2014) How microorganisms use hydrophobicity and what does this mean for human needs? Front Cell Infect Microbiol 4:112
Kristoferson LA, Bokalders V (1986) 3—Agricultural residues and organic wastes. In: Renewable energy technologies: their applications in developing countries. Bokalders
Krsmanovic M, Biswas D, Ali H, Kumar A, Ghosh R, Dickerson AK (2021) Hydrodynamics and surface properties influence biofilm proliferation. Adv Colloid Interface Sci 288:102336
Le Guennec L, Virion Z, Bouzinba-Ségard H, Robbe-Masselot C, Léonard R, Nassif X, Bourdoulous S, Coureuil M (2020) Receptor recognition by meningococcal type IV pili relies on a specific complex N-glycan. Proc Natl Acad Sci USA 117(5):2606–2612
Lehmann J, Joseph S (2024) Biochar for environmental management: science, technology and implementation. Taylor & Francis, London
Lehmann J, da Silva JP, Steiner C, Nehls T, Zech W, Glaser B (2003) Nutrient availability and leaching in an archaeological anthrosol and a ferralsol of the central amazon basin: fertilizer, manure and charcoal amendments. Plant Soil 249(2):343–357
Lehmann J, Rillig MC, Thies J, Masiello CA, Hockaday WC, Crowley D (2011) Biochar effects on soil biota–a review. Soil Biol Biochem 43(9):1812–1836
Li G, Tam L-K, Tang JX (2008) Amplified effect of Brownian motion in bacterial near-surface swimming. Proc Natl Acad Sci USA 105(47):18355–18359
Li W, Yan Z, Ren J, Qu X (2018) Manipulating cell fate: dynamic control of cell behaviors on functional platforms. Chem Soc Rev 47(23):8639–8684
Liang Y, Xu X, Yuan F, Lin Y, Xu Y, Zhang Y, Chen D, Wang W, Hu H, Ou JZ (2023) Graphene oxide additive-driven widening of microporous biochar for promoting water pollutant capturing. Carbon 205:40–53
Limoli DH, Jones CJ, Wozniak DJ (2015) Bacterial extracellular polysaccharides in biofilm formation and function. Microbiol Spectr
Liu XM, Sheng GP, Luo HW, Zhang F, Yuan SJ, Xu J, Zeng RJ, Wu JG, Yu HQ (2010) Contribution of extracellular polymeric substances (EPS) to the sludge aggregation. Environ Sci Technol 44(11):4355–4360
Liu Y, Ma S, Chen J (2018) A novel pyro-hydrochar via sequential carbonization of biomass waste: preparation, characterization and adsorption capacity. J Clean Prod 176:187–195
Liu J, Qi W, Li Q, Wang SG, Song C, Yuan XZ (2020) Exogenous phosphorus-solubilizing bacteria changed the rhizosphere microbial community indirectly. 3 Biotech 10(4):1–11
Liu Z, Wu Z, Tian F, Liu X, Li T, He Y, Li B, Zhang Z, Yu B (2023) Phosphate-solubilizing microorganisms regulate the release and transformation of phosphorus in biochar-based slow-release fertilizer. Sci Total Environ 869:161622
Lushi E, Wioland H, Goldstein RE (2014) Fluid flows created by swimming bacteria drive self-organization in confined suspensions. Proc Natl Acad Sci USA 111(27):9733–9738
MacDonald GK, Bennett EM, Potter PA, Ramankutty N (2011) Agronomic phosphorus imbalances across the world's croplands. Proc Natl Acad Sci USA 108(7):3086–3091
Martínez EJ, Rosas JG, Sotres A, Moran A, Cara J, Sánchez ME, Gómez X (2018) Codigestion of sludge and citrus peel wastes: Evaluating the effect of biochar addition on microbial communities. Biochem Eng J 137:314–325
Matsumoto S, Ohtaki A, Hori K (2012) Carbon fiber as an excellent support material for wastewater treatment biofilms. Environ Sci Technol 46(18):10175–10181
Meng J, He T, Sanganyado E, Lan Y, Zhang W, Han X, Chen W (2019) Development of the straw biochar returning concept in China. Biochar 1:139–149
Mittelviefhaus M, Müller DB, Zambelli T, Vorholt JA (2019) A modular atomic force microscopy approach reveals a large range of hydrophobic adhesion forces among bacterial members of the leaf microbiota. ISME J 13(7):1878–1882
Mohamed Zuki F, Edyvean RG, Pourzolfaghar H, Kasim N (2021) Modeling of the van der Waals forces during the adhesion of capsule-shaped bacteria to flat surfaces. Biomimetics 6(1):5
Mohanty SK, Cantrell KB, Nelson KL, Boehm AB (2014) Efficacy of biochar to remove *Escherichia coli* from stormwater under steady and intermittent flow. Water Res 61:288–296
Mu M, Liu S, DeFlorio W, Hao L, Wang X, Salazar KS, Taylor M, Castillo A, Cisneros-Zevallos L, Oh JK (2023) Influence of surface roughness, nanostructure, and wetting on bacterial adhesion. Langmuir 39(15):5426–5439
Mukherjee S, Sarkar B, Aralappanavar VK, Mukhopadhyay R, Basak BB, Srivastava P, Marchut-Mikolajczyk O, Bhatnagar A, Semple KT, Bolan N (2022) Biochar-microorganism interactions for organic pollutant remediation: challenges and perspectives. Environ Pollut 308:119609
Olubowale OH, Biswas S, Azom G, Prather BL, Owoso SD, Rinee KC, Marroquin K, Gates KA, Chambers MB, Xu A (2021) "May the force be with you!" force–volume mapping with atomic force microscopy. ACS Omega 6(40):25860–25875
Patil PV, Gurjar RM, Shaikh AJ, Balasubramanya RH, Paralikar KM, Varadarajan PV (2007) Cotton plant stalk—an alternate raw material to board industry. In: World cotton research conference, vol 4, pp 10–14
Qu J, Wei S, Liu Y, Zhang X, Jiang Z, Tao Y, Zhang G, Zhang B, Wang L, Zhang Y (2022) Effective lead passivation in soil by bone char/CMC-stabilized FeS composite loading with phosphate-solubilizing bacteria. J Hazard Mater 423:127043
Reddy KR, Xie T, Dastgheibi S (2014) Evaluation of biochar as a potential filter media for the removal of mixed contaminants from urban storm water runoff. J Environ Eng 140(12):04014043
Ruan B, Wu P, Liu J, Jiang L, Wang H, Qiao J, Zhu N, Dang Z, Luo H, Yi X (2020) Adhesion of Sphingomonas sp. GY2B onto montmorillonite: a combination study by thermodynamics and the extended DLVO theory. Colloids Surf B Biointerfaces 192:111085
Schwegmann H, Ruppert J, Frimmel FH (2013) Influence of the pH-value on the photocatalytic disinfection of bacteria with TiO2–Explanation by DLVO and XDLVO theory. Water Res 47(4):1503–1511
Shafiei-Sabet S, Hamad W, Hatzikiriakos S (2014) Ionic strength effects on the microstructure and shear rheology of cellulose nanocrystal suspensions. Cellul 21:3347–3359
Shrestha N, Wang J (2020) Water quality management of a cold climate region watershed in changing climate. J Environ Inform 35(1):56–80
Song Z, Yang S, Li P, Sun J, Xing D, Peng W, Sun F (2021) Roles of initial bacterial attachment and growth in the biofouling development on the microfiltration membrane: from viewpoints of individual cell and interfacial interaction energy. J Membr Sci 638:119723
Sun D, Hale L, Crowley D (2016) Nutrient supplementation of pinewood biochar for use as a bacterial inoculum carrier. Biol Fertil Soils 52(4):515–522
Swain MR, Laxminarayana K, Ray RC (2012) Phosphorus solubilization by thermotolerant Bacillus subtilis isolated from cow dung microflora. Agric Res 1:273–279
Thwala JM, Li M, Wong MC, Kang S, Hoek EM, Mamba BB (2013) Bacteria–polymeric membrane interactions: atomic force microscopy and XDLVO predictions. Langmuir 29(45):13773–13782
Tomczyk A, Sokołowska Z, Boguta P (2020) Biochar physicochemical properties: pyrolysis temperature and feedstock kind effects. Rev Environ Sci Biotechnol 19:191–215
Toro M, Azcon R, Barea J (1997) Improvement of arbuscular mycorrhiza development by inoculation of soil with phosphate-solubilizing rhizobacteria

to improve rock phosphate bioavailability ((sup32) P) and nutrient cycling. Appl Environ Microbiol 63(11):4408–4412
Trimurtulu, N., Rao, D., Trimurtulu, N., Amaravathi, G., 2014. Liquid microbial inoculants and their efficacy on field crops, ANGRAU. Agricultural Research Station, Amaravathi 54.
Uchimiya M (2014) Influence of pH, ionic strength, and multidentate ligand on the interaction of CdII with biochars. Acs Sustain Chem Eng 2(8):2019–2027
Vigeant MA-S, Ford RM, Wagner M, Tamm LK (2002) Reversible and irreversible adhesion of motile Escherichia coli cells analyzed by total internal reflection aqueous fluorescence microscopy. Appl Environ Microbiol 68(6):2794–2801
Vijay V, Shreedhar S, Adlak K, Payyanad S, Sreedharan V, Gopi G, Sophia van der Voort T, Malarvizhi P, Yi S, Gebert J (2021) Review of large-scale biochar field-trials for soil amendment and the observed influences on crop yield variations. Front Energy Res 9:710766
Viljoen A, Mignolet J, Viela F, Mathelié-Guinlet M, Dufrêne YF (2020) How microbes use force to control adhesion. J Bacteriol 202(12):00125–120
Wan W, Qin Y, Wu H, Zuo W, He H, Tan J, Wang Y, He D (2020) Isolation and characterization of phosphorus solubilizing bacteria with multiple phosphorus sources utilizing capability and their potential for lead immobilization in soil. Front Microbiol 11:752
Wang J, Wang S (2019) Preparation, modification and environmental application of biochar: a review. J Clean Prod 227:1002–1022
Wang Y, Hu Y, Zhao X, Wang S, Xing G (2013) Comparisons of biochar properties from wood material and crop residues at different temperatures and residence times. Energy Fuels 27(10):5890–5899
Wang Y, Zhang W, Shang J, Shen C, Joseph SD (2019) Chemical aging changed aggregation kinetics and transport of biochar colloids. Environ Sci Technol 53(14):8136–8146
Wang Z, Chen H, Zhu Z, Xing S, Wang S, Chen B (2022) Low-temperature straw biochar: sustainable approach for sustaining higher survival of B. megaterium and managing phosphorus deficiency in the soil. Sci Total Environ 830:154790
Weidenmaier C, Peschel A (2008) Teichoic acids and related cell-wall glycopolymers in gram-positive physiology and host interactions. Nat Rev Microbiol 6(4):276–287
Xiang L, Harindintwali JD, Wang F, Redmile-Gordon M, Chang SX, Fu Y, He C, Muhoza B, Brahushi F, Bolan N (2022) Integrating biochar, bacteria, and plants for sustainable remediation of soils contaminated with organic pollutants. Environ Sci Technol 56(23):16546–16566
Xu H-J, Wang X-H, Li H, Yao H-Y, Su J-Q, Zhu Y-G (2014) Biochar impacts soil microbial community composition and nitrogen cycling in an acidic soil planted with rape. Environ Sci Technol 48(16):9391–9399
Zeng Z, Xiao J, Li M, Wu J, Zhang T (2023) Degradation of phenol by immobilized alcaligenes faecalis Strain JH1 in Fe3O4-modified biochar from pharmaceutical residues. Water 15(23):4084
Zhang H, Voroney R, Price G (2015) Effects of temperature and processing conditions on biochar chemical properties and their influence on soil C and N transformations. Soil Biol Biochem 83:19–28
Zhang Y, Wayner CC, Wu S, Liu X, Ball WP, Preheim SP (2021) Effect of strain-specific biofilm properties on the retention of colloids in saturated porous media under conditions of stormwater biofiltration. Environ Sci Technol 55(4):2585–2596
Zhang Y, Liu S, Niu L, Su A, Li M, Wang Y, Xu Y (2023) Sustained and efficient remediation of biochar immobilized with Sphingobium abikonense on phenanthrene-copper co-contaminated soil and microbial preferences of the bacteria colonized in biochar. Biochar 5(1):43
Zhao R, Huang L, Peng X, Fan L, Chen S, Qin P, Zhang J, Chen A, Huang H (2023) Effect of different amounts of fruit peel-based activator combined with phosphate-solubilizing bacteria on enhancing phytoextraction of Cd from farmland soil by ryegrass. Environ Pollut 316:120602
Zheng BX, Ding K, Yang XR, Wadaan MAM, Hozzein WN, Penuelas J, Zhu YG (2019) Straw biochar increases the abundance of inorganic phosphate solubilizing bacterial community for better rape (*Brassica napus*) growth and phosphate uptake. Sci Total Environ 647:1113–1120
Zhu J, Li M, Whelan M (2018a) Phosphorus activators contribute to legacy phosphorus availability in agricultural soils: a review. Sci Total Environ 612:522–537
Zhu L, Zhao N, Tong L, Lv Y, Li G (2018b) Characterization and evaluation of surface modified materials based on porous biochar and its adsorption properties for 2, 4-dichlorophenoxyacetic acid. Chemosphere 210:734–744